Critical Waves and the Length Problem of Biology

Robert B. Laughlin
*Department of Physics, Stanford University, Stanford, CA 94305**
(Dated: March 1, 2015)

It is pointed out that the mystery of how biological systems measure their lengths vanishes away if one premises that they have discovered a way to generate linear waves analogous to compressional sound. These can be used to detect length at either large or small scales using echo timing and fringe counting. It is shown that suitable linear chemical potential waves can, in fact, be manufactured by tuning to criticality conventional reaction-diffusion with a small number substances. Min oscillations in *E. coli* are cited as precedent resonant length measurement using chemical potential waves analogous to laser detection. Mitotic structures in eucaryotes are identified as candidates for such an effect at higher frequency. The engineering principle is shown to be very general and functionally the same as that used by hearing organs.

It is not known how living things measure their lengths. This is true notwithstanding the immense progress made over the past 30 years in understanding morphogen gradients in embryogenesis.[1–6]. The problem is captured nicely by the confusion over regulation of the bicoid profile in *Drosophila*[7–11], but it is also reflected in the notorious instability, hysteresis, and lack of scalability of traditional static reaction-diffusion[12,13]. No one knows why cells are the size they are[14], why plants and animals are the size they are[15], how organs grow maintaining their proportions[16], and how some animal bodies regenerate lost limbs[17]. On the matter of length determination, per se, very little progress has been made beyond Thompson's 1917 treatise on biological form[18].

Length has a special place in biology by virtue of being a primitive quantity with units. It is not possible for living things to size themselves properly without having developed the skill of measuring these quantities as numbers and relating these numbers to each other mathematically. They require meter sticks to do this. They must fabricate these meter sticks using diffusion and motors, since they are the only biochemical elements that involve length. The relationships of these meter sticks to each other and to the lengths they measure must be precise and described by equations. This is because precise mathematical relationships among lengths are what size and shape are.

In this paper I point out that the difficulty of accounting for length relationships of parts of organisms with equations disappears instantly if the organism is premised to have discovered a way to emulate elementary physical law. In particular, one simple invention is sufficient to facilitate the measurement and construction of body plans of any shape and size one might wish in a way that is both plastic and scalable: the conversion of diffusive motion into *linear* waves using engines. The concept is general because all motion in the presence of disorder, including motion of cytoskeletal components, becomes diffusive at long time and length scales by virtue of evolving into a random walk. But if engines can transform this random walking into propagation with stable direction and speed, then signals can be beamed, like a flashlight, reflected from boundaries, and trapped.

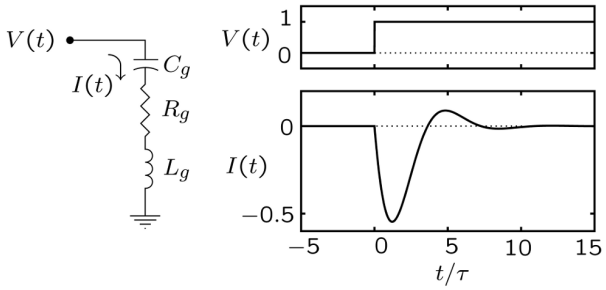

FIG. 1: Chemical amplifier described in electrical terms. The circuit components R_g, L_g and C_g all have negative values. On the right is shown the impulse response described by Eq. (1) for the special case of $R_gC_g = L_g/R_g = \tau$. The voltage step height V_0 is set to 1. The current response, plotted as a multiple of $V_0/|R_g|$, is negative and has the same shape as a neuron action potential.

Once this happens, the organism can measure lengths the same way human engineers do, by echo timing or by fringe counting and resonance. Body designs based on this strategy are inherently plastic because fixing the speed enables lengths to be laid out or detected by means of clock tick intervals, which are easy to change.

Although it is not widely known, biological systems can easily manufacture such waves using elementary reaction-diffusion chemistry similar to that at work in neuron action potentials.[19] The key is tuning the chemical reactions to the edge of an instability, an effect known in the cochlear amplifier literature as criticality.[20–22] As I shall show, this trick is so easy to implement technically that it is hard to imagine how Nature would not have exploited its tremendous engineering advantages in the struggle for survival. This obligates us to take seriously even very small hints that Nature did, in fact, discover how to do it long ago. The simple explanation for why we have found only sparse empirical evidence for such waves so far is that chemical potential waves are difficult to detect with existing laboratory techniques. The larger idea implicit in this proposed resolution of the length problem is that biological systems cannot conduct engineering without rules any more than we humans can,

so they invented some in the ancient past, and the ones that worked best turned out to be same ones we humans discovered later using reason.

I. CHEMICAL POTENTIAL WAVES

The simplest chemical length mensuration apparatus involves chemical potential waves solely. Apparati with other components, such as mechanical motors, are allowed also, but all of them necessarily have a chemical potential component by virtue of how they work.

Despite being difficult to detect, chemical potential waves are known to be pervasive in biology. The most familiar case is the neuron action potential, the electrical aspects of which make it easy to detect by primitive means, even though it is fundamentally a reaction-diffusion wave[23]. But there are also non-electrical varieties: cAMP waves in slime molds, which direct the colony's organization into fruiting bodies[24]; calcium waves, directly implicated in oogengenesis[25,26], developmental patterning[27], brain function[28–30], and cell signaling in animals[31] and plants[32]; and MinDE waves in *E. coli*, perhaps the most important of all because they are involved in a bacterial length decision[33]. All of these non-electrical versions require highly advanced technologies to see, and also required a bit of luck to find, so there is good reason to suspect that more exist and simply have not been detected yet.

The simplest way chemical reactions can manufacture waves is through stable two-terminal amplification, the fundamental basis of laser operation[34]. The observation that amplification is involved is important, for while all amplifiers exploit nonlinearities to work, there is nothing inherently nonlinear about what they do. All amplifiers become nonlinear when they are pushed to deliver large powers. It is thus not surprising that the wave signals easiest to observe in biology are often nonlinear. But amplification in the linear regime is known to occur as well, notably in hearing organs[35–40].

II. AMPLIFIERS: STABILITY AND CAUSALITY

Two-terminal amplifiers are easiest to explain by electrical analogy. Consider the circuit shown in Fig. 1. It is a conventional linear resonator, such as one might find in any radio, except that the components all have negative values. Its active component, the negative resistor, causes electric current to flow in a direction opposite to the way it normally would when voltage is applied. Such reversed flow is implicit in all Na^+-K^+ neural models, including the original one of Hodgkin and Huxley[41], but it is quite explicit in those based on tunnel diodes[42]. The all-important $C_g < 0$ causes induced current to stop flowing after a time R_gC_g. Na^+ channels achieve this cessation by plugging themselves after a time delay with

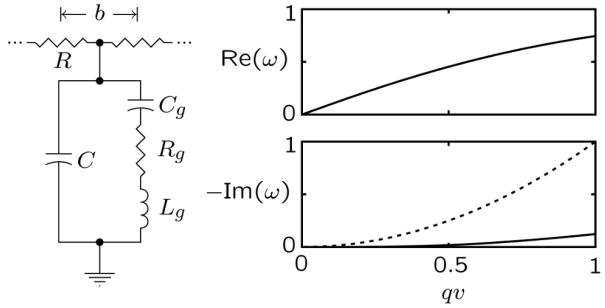

FIG. 2: Left: Illustration of a diffusive transmission line with a series of amplifiers like those in Fig. 1 placed across it. R and C represent the resistance and capacitance per unit length before the amplifier is added. The repeat distance is b. Right: Plot of the solution of Eq. (4) for the special case of $C + C_g = 0$ and $R_gC_g = L_g/R_g = \tau$. Both ω and qv are expressed as multiples of $1/\tau$. The complex numbers ω and its negative complex conjugate $-\omega^*$ are two of the three roots, the third being pure imaginary and off the top of the graph. The dashed line is the solution when the amplifiers are turned off ($C_g \to 0$).

a molecular stopper[43]. The $L_g < 0$ mainly causes a finite turn-on time L_g/R_g, but it also adjusts the circuit's after-bounce, so it corresponds to the K^+ channel of a neuron. Thus Fig. 1 is simply a linearized version of the Hodgkin-Huxley equations.

It is important that both $C_g < 0$ and $L_g < 0$ are dynamical creations of the amplifier itself, not additional postulates. It is physically impossible to make a stable amplifier without also creating, as a side effect, negative reaction. This effect is seen in lasers as a reversal of the dielectric function whenever the laser gain medium becomes amplifying[44]; but the deeper reason has nothing to do with quantum mechanics or population inversions. It is causality[45]. The current induced by a stimulating voltage can appear only after the stimulus is applied, never before. The current induced by the step voltage shown in Fig. 1 is

$$I(t) = \frac{V_0}{2\pi}\int_{-\infty}^{\infty} \frac{C_g e^{-i\omega t}}{1 - i\omega R_g C_g - \omega^2 L_g C_g}\, d\omega \qquad (1)$$

It is properly causal provided that poles of the response kernel lie in the lower half of the complex plane. This requires both C_g and L_g to be negative if R_g is.

The physical principles operating in Fig. 1 apply to all amplifiers, not just electrical ones. The denominator in Eq. (1) may be seen to be a Taylor expansion in ω truncated to second order. Such a truncation is always valid at long times, and it is equivalent to stating that the system has only two poles in the complex plane and thus has only two important mechanical degrees of freedom. Those things are therefore not model assumptions at all but generic features of amplifier response at long times. In the case of Fig. 1, the degrees of freedom are charge and current, but in general they could be anything.

III. TURING CRITICAL WAVEFUNCTION

Linear waves are produced when one places a series of such amplifiers across a diffusive transmission line, as shown in Fig. 2. This is aptly analogous to placing Na^+-K^+ amplifiers across the membrane of an axon. Substituting $V_j = V_0 \exp[i(qbj - \omega t)]$, where b is the repeat length, for the voltage on the jth site, we obtain the dispersion relation

$$\frac{2}{R}[1-\cos(qb)] - i\omega C - \frac{i\omega C_g}{1 - i\omega R_g C_g - \omega^2 L_g C_g} = 0 \quad (2)$$

When the amplifiers are turned off ($C_g \to 0$), this becomes the diffusion equation

$$Dq^2 - i\omega = 0 \qquad (D = \frac{b^2}{RC}) \quad (3)$$

in the limit of small q. But when the amplifiers are turned on, and also adjusted so that $C+C_g = 0$, Eq. (2) becomes

$$(vq)^2 - \frac{\omega^2(1 - i\omega\tau)}{1 - i\omega\tau - \omega^2\tau^2} = 0 \qquad (v = \sqrt{D/\tau}) \quad (4)$$

This is functionally equivalent to the wave equation

$$\frac{\partial^2\psi}{\partial x^2} = \frac{1}{v^2}\frac{\partial^2\psi}{\partial t^2} \qquad (v = \sqrt{D/\tau}) \quad (5)$$

where ψ is any one of the dynamical variables, in the regime $qv < 0.5/\tau$. The expression for the velocity v is the Luther equation[46]. The full solution Eq. (4) is plotted in Fig. 2.

This wave equation is equivalent to the Turing reaction-diffusion equations

$$\begin{aligned} \frac{\partial X}{\partial t} &= \frac{1}{\tau}Z + D\frac{\partial^2 X}{\partial x^2} \\ \frac{\partial Y}{\partial t} &= \frac{1}{\tau}Z \\ \frac{\partial Z}{\partial t} &= \frac{1}{\tau}(X - Y - Z) \end{aligned} \quad (6)$$

It could thus easily be achieved with chemical reactions among three substances. It is also easily generalized to three dimensions. In fact, the principle behind Eq. (4) is so general that it applies to any conservative diffusive phenomenon, chemical, electrical or mechanical, at any length or time scale, regardless of details. For this reason, it is a competitive candidate for how living things might measure their lengths *generally*.

Stabilization of the wave velocity in these systems is achieved through two fine-tunings. One is equality of the capacitive and inductive times. This is a matter of amplifier design and is achieved in the case of neurons by having the right mix of Na^+ and K^+ channels. The other is cancellation of the capacitances, a result achieved in practice by slowly increasing the number of amplifiers in the membrane until the system begins to oscillate a little. Such oscillations are routinely observed emanating from the ear[47]. A similar phenomenon has been reported at the surface membranes of yeast[48].

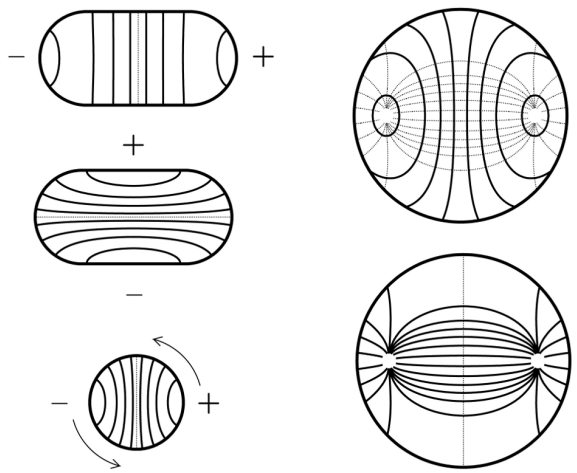

FIG. 3: Left: Solutions of Eq. (7) with Neumann boundary conditions for a pill-shaped cavity, as appropriate for a bacterium. Hemispherical end caps of radius a are attached to a cylinder of length $2.2\,a$. The top shows a contour plot of the lowest eigenfunction, which corresponds to an axially symmetric pole-to-pole sloshing. It occurs at $\omega_n = 0.88v/a$. Below that are contour plots of first longitudinally symmetric mode, which corresponds to a steady migration around the perimeter along a path perpendicular to the axis. It occurs at $\omega_n = 1.91v/a$. This mode is degenerate with a mirror-reflected one that rotates in the opposite direction. Right: Solution of Eq. (7) for a spherical cavity with mixed boundary conditions ($\hat{\mathbf{n}}\cdot\nabla\phi_n = -0.51\phi_n$). The top shows a contour plot of the lowest eigenfunction. The dotted lines, reproduced as solid lines below, are trajectories perpendicular to the contour lines.

IV. LENGTH MEASUREMENT USING CAVITY RESONANCE

The simplest strategy for measuring length with manufactured waves is detecting mode resonances in a cavity. This is illustrated in the case of 3-dimensional waves in Fig. 3. The allowed oscillations of a cavity are found by substituting a harmonic solution $\psi(\mathbf{r},t) = \phi_n(\mathbf{r})\exp(-i\omega_n t)$ into Eq. (5) and solving the Helmholtz equation

$$\nabla^2\phi_n + (\omega_n/v)^2\,\phi_n = 0 \quad (7)$$

with Neumann boundary conditions ($\hat{\mathbf{n}}\cdot\nabla\phi_n = 0$), as appropriate for a substance that is conserved and cannot

flow in or out through the walls. Solutions exist only for certain discrete eigenfrequencies ω_n. The values of these and the spatial behavior of their corresponding eigenfunctions ϕ_n sense the size and shape of the cavity. The eigenfunction ϕ_n corresponding to the lowest of eigenfrequency shown in in Fig. 3 describes to the observed MinDE wave motion in *E. coli*, although details differ.

To actually excite eigenmodes of a cavity it is necessary provide the amplifying medium with a gain peak. This is achieved most simply in the case of the example of Fig. 2 by attaching a second resonant circuit, as shown in Fig. 4. This effectively makes the amplifying resistor slightly frequency dependent, per

$$\frac{1}{R_g} \to \frac{1}{R_g}\left\{1 + f_0\left[\frac{-i\omega\tau_0}{1 - i\omega\tau_0 - (\omega/\omega_0)^2}\right]\right\} \qquad (8)$$

where $\tau_0 = R'_g C'_g$, $\omega_0 = (L'_g C'_g)^{-1/2}$ and $f_0 = R_g/R'_g$. Modifying R_g in this way is physically equivalent to humming a tone in a closed room: The tone is ω_0, the loudness is f_0, and the time between successive breaths is τ_0. The corresponding reaction-diffusion equations are

$$\begin{aligned}
\frac{dX}{dt} &= D\frac{\partial^2 X}{\partial x^2} + \frac{1}{\tau}Z \\
\frac{dY}{dt} &= \frac{1}{\tau}Z \\
\frac{dZ}{dt} &= \frac{1}{\tau}(X - Y - Z + f_0 Z') \\
\frac{dY'}{dt} &= \frac{1}{\tau_0}Z' \\
\frac{dZ'}{dt} &= \omega_0^2\tau_0\big[Z - Y' - (1 + f_0)Z'\big] \qquad (9)
\end{aligned}$$

When modified in this way the system becomes a textbook laser oscillator. As shown in Fig. 4, cavity modes with frequencies ω_n in the region of net gain grow exponentially and saturate the amplifier, meaning they eat up all the power available. In biological terms we would say that a nonlinearity chokes off the exponential growth and causes it to plateau. Laser saturation reduces the gain according to the approximate formula

$$f_0 \longrightarrow f = \frac{f_0}{1 + P/P_0} \qquad (10)$$

where P is the power delivered and P_0 is a parameter characteristic of the medium. P continues to increase until $\mathrm{Im}(\omega)$ becomes zero, as shown in Fig. 4, for the mode with the highest native gain. This implies that all the other modes in the saturated state have negative gain and die away. This winner-take-all competition for the available energy causes the system to oscillate in one mode rather than many.

The frequency and magnitude of the saturated oscillation both measure the cavity length. The coarse-grained measurement is the discrete frequency jumping that occurs as one mode after another becomes dominant as the cavity is lengthened. The power P of the victorious mode is also modified by the length adjustment through the medium's gain profile, as shown in Fig. 4. The saturated power thus provides a fine-tuning measurement of length.

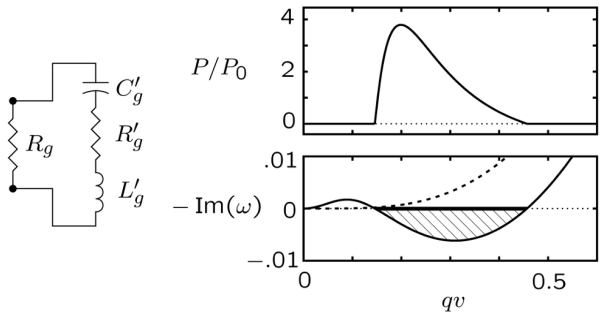

FIG. 4: Left: Illustration of the modification of R_g required to introduce a gain peak into the transmission line of Fig. 2, as described by Eq. (8). Lower Right: Correction to dispersion relation of Fig. 2 resulting from the values $\omega_0 = 0.2/\tau$, $f_0 = 0.1$, and $\tau_0 = 10\tau$. Only the imaginary part of ω is shown because the correction to the real part is negligible. Hatching indicates the region of oscillation. Here saturation, described by Eq. (10), pushes $\mathrm{Im}(\omega)$ to zero. The dashed line shows the $C'_g \to 0$ behavior. Both ω and qv are expressed as multiples $1/\tau$. Upper Right: Power produced at saturation, per Eq. (10).

V. PRECEDENT IN BACTERIA

Gain, oscillation and saturation have all been observed experimentally for MinDE oscillations in *E. coli*.[49]. Fluorescence tagging experiments have revealed that MinD molecules flock together from one end of the bacterium to the other with a round-trip travel time of about 40 seconds. Disabling expression of FtsZ, a protein required for septation and division, causes the bacterium to grow very long and exhibit a preferred MinD wavelength of approximately 10 μm, or about twice the length at which it normally divides[49]. Both standing waves and traveling waves are observed in these long mutants, depending on circumstances.[49,50] The system can also flip unstably between the two when the boundary conditions are changed. When the bacterium divides, the oscillation bifurcates unstably and then settles down with a higher frequency, just as a laser would[51]. The increase is measured to be a factor of 1.5, whereas a factor of 2 would be expected of perfectly linear waves.

There is no direct evidence that the bacteria oscillate for the purpose of measuring their lengths absolutely, nor is there any direct evidence that oscillations are universally present in all bacteria. One knows for certain only that *E. coli* use Min oscillations are part of the machinery for determining their midpoint for division, and that

a MinD homolog in *B. subtilis* has been observed to form static patterns that do not oscillate.[52]

However, circumstantial evidence is abundant. The existence of Min oscillations clearly demonstrates that chemical reactions actually present in a bacterium have the ability to manufacture chemical waves and trap them. Nature presumably created this machinery for some purpose. Min oscillations are known to involve only a small number of substances. The exact number is controversial, but the reactions are typically modeled with four or five, the same as in Eqs. (9).[53–57]. Existing experiments are not sufficiently detailed to distinguish among these models, but elementary reaction-diffusion is central to all of them, and all become similar to Eqs. (9) when linearized. The fundamental simplicity of the reactions was indicated early on by identification of MinCDE operon damage as the cause of the minicell mutation in *E. coli*[58,59], but it is now corroborated by experiments *in vitro* showing both oscillations and spatial waves occurring in system containing only MinD, MinE, a lipid membrane, and ATP[60–62]. The frequencies and lengths observed in these experiments do not agree with those observed in real bacteria, but this is not surprising given how finely tuned a reaction-diffusion system must be to measure lengths accurately. They are like a watch with a corrupted regulator: It still ticks, but it does not keep time.

It is not important that the Min amplifier machinery resides in or near the cell membrane[63,64]. For length measurement purposes, this machinery is adiabatically equivalent to Eq. (5), meaning that it can be slowly deformed into scalar waves trapped in the bacterial body without changing its functionality. The corresponding wave speed v is about 0.15 μm/sec, the same as slow calcium waves.

The wave principle also has potential bearing on the overall shape of bacteria, most of which are cylinders of fixed width. The reasons for preferring this shape are not presently known.[65] To measure the width of the body with a wave, one must excite the first azimuthal eigenmode of Eq. (5), also shown in Fig. 3. This corresponds to a motion around the perimeter perpendicular to the body axis. This mode is necessarily doubly degenerate so long as the body is exactly cylindrical, so the corresponding form would not automatically be a cylinder unless the symmetry is broken, meaning that either right-handed or left-handed motion is preferred. This is a different issue from the handed spiral structures reported in bacterial walls[66] because it requires also breaking of time-reversal symmetry, as occurs in a magnet. Such symmetry breaking is known to occur in *E. coli*, where it manifests itself through preferred swimming handedness on glass slides, an effect attributable to a preferred rotation direction of the flagellum.[67,68]

The shape-regulating protein MreB has recently been observed to execute motion circumferential and perpendicular to the body axis in *B. subtilis*[69–71]. The experiments employ difficult sub-wavelength optical microscopy, and some details remain controversial. The reported azimuthal velocities range from 7 nm/sec to 50 nm/sec, and one group reports a handedness bias while another rules it out. However, there is general agreement that MreB aggregates into small patches and that these translocate along the cell wall in a direction accurately perpendicular to the body axis.

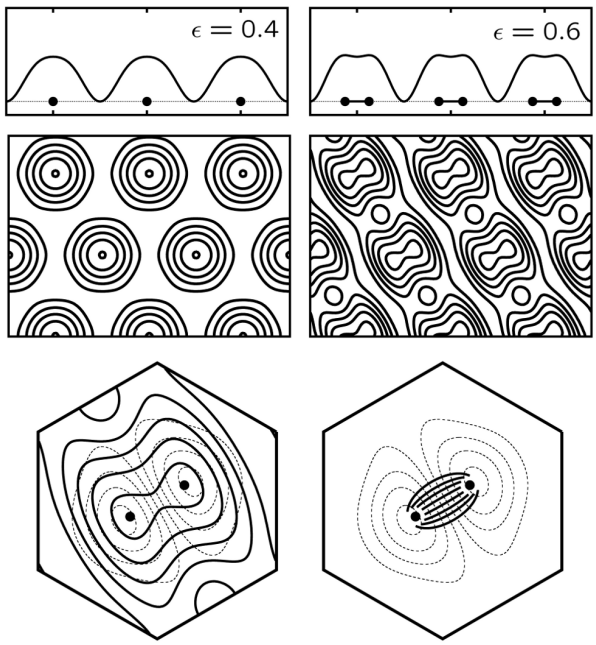

FIG. 5: Illustration of standing wave syncytium. Top: Plot of the time average of $|\psi(x,t)|^2 = |\cos(\omega x/v)\,\cos(\omega t) + \epsilon \sin(2\omega x/v)\,\cos(2\omega t)|^2$ at fixed frequency ω and wave speed v for two different values of ϵ. This shows how a standing wave grating can be made to split centrosome locations by increasing the amplitude of its first harmonic. Middle: The same quantity for the two-dimensional case expressed as a contour plot. The wavefunction is a "twinkling eyes" superposition of three plane waves at frequency ω and three more at 2ω.[74] Bottom: Contour in the hexagonal unit cell showing phase-locked signal contours of ψ and spindles constructed perpendicular to them, as in Fig. 3.

In the context of mensuration it is not important whether the patch motion involves cell wall synthesis, as the experiments seem to suggest it does. The principles by which diffusion is converted to wave motion are so general that they apply equally well to polymerization.

VI. EUCARYOTES: SPINDLES AND SYNCYTIA

Anything one says about eucaryotic size and shape control is necessarily speculative because so little definitive is known about it. However, the physical principles of resonant trapping are so simple and general that one might reasonably guess that they apply also to eucaryotic cells.

Fig. 3 also shows the solution of Eq. (7) for a spherical cavity, as might be appropriate for a eucaryotic cell. Everything is the same as for the pill-shaped cavity except for the boundary conditions, which we force to be mixed, thus pushing the antinode from the cell surface into the interior. Mixed boundary conditions are appropriate for amplification machinery that resides partly in bulk interior and partly on or near the membrane. Fig. 3 also shows trajectories generated by the rule of everywhere going downhill in the wavefunction gradient. The similarity to the mitotic spindle is unmistakable. Thus were an oscillating chemical potential field providing the navigation instructions for microtuble assembly, it would account quantitatively for (1) the location of centrosomes (the antinodes), (2) the existence and location of the metaphase plate, (3) the choice of a particular orientation for this plate, (4) the initiation and termination microtubules at the centrosomes, (5) their intersection at right angles with the metaphase plate, (6) their outward bulging at the plate, (7) the oblique angle formed between backward-going microtubules and the cell membrane, and (8) the observed scaling of the spindle assembly with cell size[72,73].

Waves also have the potential to account for the organization of structures without cell membranes. Fig. 5 shows a simple model of a syncytium made with standing waves. This specific construction uses three waves oriented at a physical angle $2\pi/3$ with respect to each other and also oscillating $2\pi/3$ out of phase with each other in time so as to create a "twinkling eyes" dynamical pattern.[74] The recipe for locating the spindles is the same as in Fig. 3. The equations used to generate Fig. 5 are much too primitive to describe an actual syncytium, among other reasons because the nuclei in real syncytia are not (cannot be) hexagonally arranged and because they have cytoskeletal structures where the cell membranes would normally have been. Nonetheless Fig. 5 shows how standing waves can create organizational patterns beyond the immediate neighborhood of a specific nucleus, and thus how they might organize larger multicellular eucaryotic structures. There are some additional potential benefits, such as providing a natural signal to synchronize mitotic division and automatically scaling structures in a syncytial embryo to egg size.

VII. CONCLUSION: STATIC VERSUS DYNAMIC REACTION-DIFFUSION

Dynamic reaction-diffusion is not a novel length mensuration method so much as an engineering advance over an older, more primitive one. When implemented at the molecular level, it uses exactly the same chemistry that static reaction-diffusion does but simply manages time differently. An apt analogy would be the time management that distinguishes the Internet from the telegraph. Both use electricity to work, but the latter uses it more cleverly and is thus vastly more powerful. Dynamic mensuration is thus fully compatible with experimental evidence that small organisms use the static version often if the latter is imagined to be vestigial.[75–77]

The crucial engineering advantage of dynamic mensuration over the static variety is plasticity. To measure out a length with an elementary diffusive morphogen one must balance a uniform destruction rate against a diffusion constant, a strategy that works perfectly well so long as the design is fixed. But if one wishes to change the design, one must modify the diffusion constant, the destruction rate, or both, making sure that the latter remains uniform. If, on the other hand, one tunes the chemical reactions to manufacture waves with a fixed speed, lengths can be easily adjusted up or down simply by changing frequencies of stimulating oscillators. These need not be located in any particular place, for standing waves are rigid and thus insensitive to the location of their stimulus, an effect familiar from the operation of musical instruments. Thus the difficult hardware design need only be done once. The hardware can then be used again and again to measure out lengths of any size one likes, even with the latter changing on the fly in response to external events not encrypted in the genes.

The other important advantage of dynamic mensuration is generalizability. Once the concept of turning diffusion into waves using amplifiers is discovered, it is very easy to imagine going by small steps to the invention of a sophisticated organ like the cochlea, which uses the same engineering principles but exploits mechanical diffusion, not chemical diffusion. It is similarly easy to imagine going by small steps to the invention of neurons, which involve the same circuitry but with the amplifier gain turned up to make the propagating pulse nonlinear, and in which the underlying diffusive motion is electrical, not chemical. Diffusion is a very general physical phenomenon that results when when motion becomes disorganized. The trick of reversing the descent into diffusive chaos using engines thus has applicability far beyond basic chemistry.

It is not a great concern that direct biochemical evidence for dynamic length measurement is thin. Bacteria, in particular, are very ancient, and it perfectly reasonable that they should employ both old and new technologies to form their bodies. But the more insightful observation is that laboratory detection of chemical potential oscillations is difficult and requires significant signal strength and integration time to do. Oscillations in other organisms might simply have not been found yet or be too weak or rapid to see easily. The diffusion constants of MinD and MinE have been measured *in vivo* by fluorescence correlation spectroscopy to be roughly $D = 10\mu\text{m}^2/\text{sec}$[78]. An amplifier time of $\tau = 10^{-3}$ sec, a number characteristic an ion channel protein, gives a maximum propagation velocity of $v = (D/\tau)^{1/2} = 100\ \mu$m/sec, the speed of a fast calcium wave. For a bacterium 3μm long, this gives a round-trip transit time of 0.06 sec. Even faster speeds are possible with electrolyte ions, for which (ambipolar) diffusion constants are D $\cong 1000\ \mu\text{m}^2/\text{sec}$.

Acknowledgments

This work was supported by the National Science Foundation under Grant No. PHY-1338376.

* R. B. Laughlin: `http://large.stanford.edu`

[1] C. Nüsslein-Volhard, "The Identification of Genes Controlling Development in Flies and Fishes (Nobel Lecture)," Angew. Chem. Int. Ed. Engl. **35**, 2176 (1996).

[2] A. Stathopoulos and D. Iber, "Studies of Morphogens: Keep Calm and Carry On," Development **140**, 4119 (2013).

[3] S. Sick, S. Reinker, J. Timmer, and T. Schlake, "WNT and DKK Determine Hair Follicle Spacing Through a Reaction-Diffusion Mechanism," Science **314**, 1447 (2006).

[4] A. Economou *et al.*, "Periodic Stripe Formation by a Turing Mechanism Operating at Growth Zones in the Mammalian Palate," Nat. Gen. **44**, 348 (2011).

[5] R. Sheth *et al.*, "*Hox* Genes Regulate Digit Patterning By Cntrolling the Wavelength of a Turing-Type Mechanism," Science **338**, 1476 (2012).

[6] P. Müller *et al.*, "Differential Diffusivity of Nodal and Lefty Underlies a Reaction-Diffusion Patterning System," Science **336**, 721 (2012).

[7] T. Gregor, A. P. McGregor, and E. F. Wieschaus, "Shape and Function of the Bicoid Morphogen Gradient in Dipteran Species With Different Sized Embryos," Devel. Biol. **316**, 350 (2008).

[8] A. Spirov *et al.*, "Formation of the Bicoid Morphogen Gradient: An mRNA Gradient Dictates the Protein Gradient," Development **136**, 605 (2009).

[9] H. D. Lipshitz, "Follow the mRNA: a New Model For Bicoid Gradient Formation," Nat. Rev. Mol. Cell Bio. **10**, 509 (2009).

[10] O. Grimm, M. Coppey, and E. Wieschaus, "Modeling the Bicoid Gradient," Development **137** 2253 (2010).

[11] D. Cheung, C. Miles, M. Kreitman, and J. Ma, "Adaptation of the Length Scale and Amplitude of the Bicoid Gradient Profile to Achieve Robust Patterning in Abnormally Large *Drosophila melanogaster* Embryos," Development **141**, 124 (2014).

[12] A. J. Koch and H. Meinhardt, "Biological Pattern Formation: From Basic Mechanisms to Complex Structures," Rev. Mod. Phys. **66**, 1481 (1994).

[13] J. E. Pearson, "Complex Patterns in a Simple System," Science **261**, 189 (1993).

[14] W. F. Marshall *et al.*, "What Determines Cell Size?" BMC Biol. **10**, 101 (2012).

[15] H. F. Nijhout, "The Control of Body Size in Insects," Devel. Biol. **261**, 1 (2013).

[16] B. Z. Stanger, "Organ Size Determination and the Limits of Regulation," Cell Cycle **7**, 318 (2008).

[17] R. S. King and P. A. Newmark, "The Cell Biology of Regeneration," J. Cell. Biol. **196**, 553 (2012).

[18] D. W. Thompson, (1992) *On Growth and Form: The Complete and Revised Edition* (Dover, New York, 1992).

[19] A. M. Turing, "The Chemical Basis of Morphogenesis," P. R. Soc. London B **237**, 37 (1952).

[20] T. Gold, "Hearing. II. The Physical Basis of the Action of the Cochlea," P. R. Soc. Lond B **135**, 492 (1948).

[21] S. Camalet, T. Duke, F. Jülicher, and J. I. Prost, "Auditory Sensitivity Provided By Self-Tuned Critical Oscillations of Hair Cells," Proc. Natl. Acad. Sci USA **97**, 3183 (2000).

[22] A. J. Hudspeth, F. Jülicher, and P. Martin, "A Critique of the Critical Cochlea: Hopf - A Bifurcation - Is Better Than None," J. Neurophysiol. **104**, 1219 (2010).

[23] A. W. Scott, "The Electrophysics of a Nerve Fiber," Rev. Mod. Phys. **47**, 487 (1975).

[24] A. Goldbeter, "Oscillations and Waves of Cyclic AMP in *Dictyostelium*: A Prototype For Spatio-Temporal Organization and Pulsatile Intercellular Communication," Bull. Math. Biol. **58**, 1095 (2006).

[25] L. F. Jaffe, "Calcium waves," Phil. Trans. Roy. Soc. B **363**, 1311 (2008).

[26] L. F. Jaffe, "Organization of Early Development By Calcium Patterns," Bioessays **21**, 567 (1999).

[27] M. Whitaker and J. Smith, "Introduction. Calcium Signals and Developmental Patterning," Phil. Trans. Roy. Soc. B, **363**, 1307 (2008).

[28] T. A. Weissman, P. A. Riqueime, L. Ivic, A. C. Flint, and A. R. Kriegstein, "Calcium Waves Propagate Through Radial Glial Cells and Modulate Proliferation in the Developing Neocortex,m" Neuron **43**, 647 (2004).

[29] E. Scemes and C. Giaume, "Astrocyte Calcium Waves: What They Are and What They Do," Glia **54**, 716 (2006).

[30] N. Kuga, T. Sasaki, Y. Takahara, N. Matsuki, and Y. Ikegaya, "Large-Scale Calcium Waves Traveling Through Astrocytic Networks *in vivo*," J. Neurosci. **31**, 2607 (2011).

[31] M. Junkin, Y. Lu, J. Long, P. A. Deymier, J. B. Hoying, and P. K. Wong, "Mechanically Induced Intercellular Calcium Communication in Confined Endothelial Structures," Biomat. **34**, 2049 (2013).

[32] W.-G. Choi, M. Toyota, S.-H. Kim, R. Hilleary, and S. Gilroy, "Salt Stress-Induced Ca^{2+} Waves Are Associated With Rapid, Long-Distance Root-to-Root Signaling in Plants," Proc. Natl. Acad. Sci. **111**, 5497 (2014).

[33] P. Lenz and L. Sogaard-Anderson, "Temporal and Spatial Oscillations in Bacteria," Nat. Rev. Microbiol. **9**, 565 (2011).

[34] A. E. Siegman, *Lasers* (University Science Books, Herdon, VA, 1986)

[35] J. E. Gale and J. F. Ashmore, "An Intrinsic Frequency Limit to the Cochlear Amplifier," Nature **389**, 63 (1997).

[36] J. Ashmore *et al.*, "The Remarkable Cochlear Amplifier," Hearing Res. **266**, 1 (2010).

[37] G. A. Manley, "Evidence For an Active Process and a Cochlear Amplifier in Nonmammals," J. Neurophysiol. **86**, 541 (2001).

[38] B. Warren, A. N. Lukashkin, and I. J. Russell, "The Dynein-Tubulin Motor Powers Active Oscillations and Amplification in the Hearing Organ of the Mosquito," P. R. Soc. B **277**, 1761 (2010).

[39] N. Mhatre and D. Robert, "A Tympanal Insect Ear Exploits a Critical Oscillator For Active Amplification and

Tuning," Curr. Biol. **23**, 1952 (2013).
[40] E. C. Mora, A. Cobo-Cuan, F. Macías-Escrivá, M. Pérez, M. Nowotny, and M. Kössl, "Mechanical Tuning of the Moth Ear: Distortion-Product Otoacoustic Emissions and Tympanal Vibrations," J. Exp. Biol. **216**, 3863 (2013).
[41] A. L. Hodgkin and A. F. Huxley, "A Quantitative Description of Membrane Current and Its Application to Conduction and Excitation of Nerve," J. Physiol. **117**, 500 (1952).
[42] R. Fitzhugh, "Mathematical Models of Excitation and Propagation in Nerve," in *Biological Engineering*, ed. by H. P. Schwan (McGraw Hill, New York, 1969).
[43] A. L. Goldin, "Mechanisms of Sodium Channel Inactivation," Curr. Opin. Neurobiol. **13**, 284 (2003).
[44] E. Desurvire, "Study of the Complex Atomic Susceptibility of Erbium-Doped Fiber Amplifiers," J. Lightwave Technol. **8**, 1517 (1990).
[45] J. S. Toll, "Causality and the Dispersion Relation: Logical Foundations," Phys. Rev. **104**, 1760 (1956).
[46] K. Showalter and J. J. Tyson, "Luther's 1906 Discovery of Chemical Waves," J. Chem. Ed. **64**, 742 (1987).
[47] D. T. Kemp, "Stimulated Acoustic Emissions From Within the Human Auditory System," J. Acoust. Soc. Am. **54**, 1386 (1978).
[48] A. E. Pelling, S. Dehati, E. B. Gralla, J. B. Valentine, and J. K. Gimzewski, "Local Nanomechanical Motion of the Cell Wall of *Saccharomyes cerevisiae*," Science **305**, 1147 (2004).
[49] D. M. Raskin and P. A. J. de Boer, "Rapid Pole-to-Pole Oscillations of a Protein Required For Directing Division to the Middle of *Escherichia coli*," Proc. Natl. Acad. Sci. USA **96**, 4971 (1999).
[50] G. Meacci, *Min Oscillations in Escherichia Coli* (VDM, Saarbrüken, 2009).
[51] J. R. Juarez and W. Margolin, "Changes in the Min Oscillation Pattern Before and After Cell Birth," J. Bacteriol. **192**, 4134 (2010).
[52] A. L. Marston, H. B. Thomaides, D. H. Edwards, M. E. Sharpe, and J. Errington, Polar Localization of the MinD Protein of *Bacillus subtilis* and Its Role in Selection of the Mid-Cell Division Site," Genes Devel. **12**, 3419 (1998().
[53] M. Howard, A. D. Rutenberg, and S. De Vet, "Dynamic Compartmentalization of Bacteria: Accurate Division in *E. coli*," Phys. Rev. Lett. **87**, 278102 (2001).
[54] H. Meinhardt and P. A. J. de Boer, "Pattern Formation in *Escherichia coli*: A Model For the Pole-to-Pole Oscillations of Min Proteins and the Localization of the Division Site," Proc. Natl. Acad. Sci. USA **98**, 14202 (2001).
[55] K. C. Huang, Y. Meir, and N. S. Wingreen, "Dynamic Structures in *Escherichia coli*: Spontaneous Formation of MinE Rings and MinD Polar Zones," Proc. Natl. Acad. Sci. (USA) **100**, 12724 (2003).
[56] M. Bonny, E. Fischer-Friedrich, M. Loose, P. Schwille, and K. Kruse, "Membrane Binding of MinE Allows For a Comprehensive Description of Min-Protein Pattern Formation," PLOS Comp. Biol. **9**, e1003347 (2013).
[57] J. Halatek and E. Frey, "Effective 2d Model Does Not Account For Geometry Sensing By Self-Organized Proteins Patterns," Proc. Natl. Acad. Sci. USA **111**, E1817 (2014).
[58] H. I. Adler, W. D. Fisher, A. Cohen, and A. A. Hardigree, "Miniature *Escherichia coli* Cells Deficient in DNA," Proc. Natl. Acad. Sci. (USA) **57**, 321 (1967).
[59] P. A. J. de Boer, R. E. Crossley, and L. I. Rothfield, "A Division Inhibitor and a Topological Specificity Factor Coded For by the Minicell Locus Determine Proper Placement of the Division Septum in *E. coli*," Cell **56**, 641 (1989).
[60] M. Loose, E. Fischer-Friedrich, J. Ries, K. Kruse, and P. Schwille, "Spatial Regulators For Bacterial Cell Division Self-Organize into Surface Saves *in Vitro*," Science **320**, 789 (2008).
[61] V. Ivanov and K. Mizuuchi, "Multiple Modes of Interconverting Dynamic Pattern Formation by Bacterial Cell Division Proteins," Proc. Natl. Acad. Sci. (USA) **107**, 8071 (2010).
[62] J. Schweizer, M. Loose, M. Bonny, K. Kruse, I Mönch, and P. Schwille, "Geometry Sensing By Self-Organized Protein Patterns," Proc. Natl. Acad. Sci. (USA) **109**, 15283 (2012).
[63] Z. Hu, E. P. Gogol, and J. Lutkenhaus, Dynamic Assembly of MinD on Phospholipid Vesicles Regulated by ATP and MinE," Proc. Natl. Acad. Sci. (USA) **99**, 6761 (2002).
[64] L. L. Lackner, D. M. Raskin, and P. A. J. de Boer, "ATP-Dependent Interactions Between *Escherichia coli* Min Proteins and the Phospholipid Membrane P*in vitro*," J. Bacteriol. **185**, 735 (2003).
[65] K. D. Young, "Bacterial Shape: Two-Dimensional Questions and Possibilities," Annu. Rev. Microbiol. **64**, 223 (2010).
[66] K. C. Huang, D. W. Ehrhardt, and J. W. Shaevitz, "The Molecular Origins of Chiral Growth in Walled Cells," Curr. Opin. Microbiol. **15**, 1 (2012).
[67] W. R. DiLuzio, L. Turner, M. Mayer, P. Garstecki, D. B. Weibel, H. C. Berg, and G. M. Whitesides, "*Escherichi coli* Swim on the Right-Hand Side," Nature **435**, 1271 (2005).
[68] E. Lauga, W. R. DiLuzio, G. M. Whitesides, and M. A. Stone, "Swimming in Circles: Motion of Bacteria Near Solid Boundaries," Biophys. J. **90**, 400 (2006).
[69] E. C. Garner, R. Bernhard, W. Wang, X. Zhuang, D. Z. Rudne, and T Mitchison, "Coupled, Circumferential Motions of the Cell Wall Synthesis Machinery and MreB Filaments in *B. subtilis*," Science **333**, 222 (2011).
[70] J. Domínguez-Escobar, A. Chastanet, A. H. Crevenna, V. Fromion, R. Wedlich-Söldner, and R Carballido-López, "Precessive Movement of MreB-Associated Complexes in Bacteria," Science **333**, 225 (2011).
[71] S. van Teeffelen, S. Wang, L. Furchgott, K. C. Huang, N. S. Wingreen, J. W. Shaevitz, and Z. Gital, "The Bacterial Actin MreB Rotates, and Rotation Depends on Cell-Wall Assembly," Proc. Natl. Acad. Sci. **108**, 15882 (2011).
[72] J. Hazel *et al.*, "Changes in Cytoplasmic Volume Are Sufficient to Drive Spindle Scaling," Science **342**, 853 (2013).
[73] M. C. Good, M. D. Vahey, A. Skandarjah, D. A. Fletcher, and R. Heald, "Cytoplasmic Volume Modulates Spindle Size During Embryogenesis," Science **324**, 856 (2013).
[74] L. Yang and I. R. Epstein, "Oscillatory Turing Patterns in Reaction-Diffusion Systems With Two Coupled Layers," Phys. Rev. Lett. **90**, 178303 (2003).
[75] H. Meinhardt H, "Models of Biological Pattern Formation: From Elementary Steps to the Organization of Embryonic Axes," Curr. Top. Dev. Biol. **81**, 1 (2008).
[76] S. Kondo and T. Miura, "Reaction-Diffusion Model as a Framework for Understanding Biological Pattern Formation," Science **329**, 1616 (2010).
[77] D. M. Umulis and H. G. Othmer, "Mechanisms of Scaling in Pattern Formation," Development **140**, 4830 (2013).
[78] G. Meacci, J. Ries, E. Fischer-Friedrich, N. Kahya, P. Schwille, and K. Kruse, "Mobility of Min-proteins in *Escherichia coli* Measured by Fluorescence Correlation Spectroscopy," Phys. Biol. **3**, 255 (2006).